IEEE Access
Multidisciplinary ⋮ Rapid Review ⋮ Open Access Journal

Received September 5, 2020, accepted September 8, 2020, date of publication September 11, 2020,
date of current version September 25, 2020.

Digital Object Identifier 10.1109/ACCESS.2020.3023485

Low-Light Image Enhancement via Pair of Complementary Gamma Functions by Fusion

CHANGLI LI[1], SHIQIANG TANG[1], JINGWEN YAN[2], AND TENG ZHOU[2]

[1]Advanced Signal and Image Processing, Learning, and Engineering Laboratory (A Simple Lab.), College of Computer and Information Engineering, Hohai University, Nanjing 211100, China

[2]College of Engineering, Shantou University, Shantou 515063, China

Corresponding author: Changli Li (charlee@hhu.edu.cn)

This work was supported in part by the Open Fund of Guangdong Provincial Key Laboratory of Digital Signal and Image Processing Technology, and in part by the National Natural Science Foundation of China under Grant 61871174.

ABSTRACT Enhanced images by the traditional gamma correction (GC) method still have low contrast within high illuminance regions. In order to enhance the visibility in dark regions and simultaneously achieve high contrast in bright regions for low-light images, this paper proposes a novel method via a pair of complementary gamma functions (PCGF) by image fusion. We first define PCGF and then show its outstanding potential for low-light image enhancement by some preliminary experimental results. In order to release its performance and verify its effectiveness, we further design a simple enhancement method for low-light images based on it by an elaborately designed fusion strategy. Two input images for fusion are derived from the enhanced image by PCGF and that by proposed sharpening method, respectively. Experiments show that our proposed method can significantly enhance the detail and improve the contrast of low-light image. The qualitative experiment results show that the proposed method is effective and the comparative quantitative assessment shows that it outperforms other state-of-the-art methods.

INDEX TERMS Gamma correction (GC), CRT gamma, pair of complementary gamma functions, low-light image enhancement, image dehazing, underwater image restoration.

I. INTRODUCTION

High quality images play an important role in object detection [1], image classification [2], and saliency detection [3] and so on. However, it is generally difficult for us to obtain high quality images because of the limitations of image acquisition technology and environment. Under the condition of low illuminance, due to the surrounding environment or lack of self-exposure, images captured by optical imaging devices are overall visually dark, blurred in detail and poor visible. Many methods, such as histogram-based methods [4]–[12], Retinex-based methods [7], [13]–[22] and fusion-based methods [23]–[26], have been proposed to enhance low-light images.

Histogram-based methods are based on the modification of histogram to enhance the contrast of images with low illumination. Histogram equalization (HE) [4] and contrast-limited adaptive histogram equalization (CLAHE) [5] are commonly used due to their effectiveness in improving image contrast and detail, but their drawbacks are over-enhancement and the introduction of artifacts in color images. To overcome these defects, in [6] a contrast enhancement method using layered difference representation of 2D histograms is proposed. In [7], a hybrid histogram modification method is proposed by combining gamma correction and traditional histogram equalization. However, the enhanced images look filled with gloom darkness. In [8] a so-called contextual and variational contrast enhancement (CVC) method is proposed by a histogram mapping which emphasizes large gray-level differences. However, these methods will meet difficulties when dealing with very dark regions because of the limitation of stretching range.

Retinex-based algorithms (such as SSR [14], MSR [15], and MSRCR [16]) are effective for image processing. However, the enhanced result for low-light image is often gray-out. In order to solve this problem, researchers have made much improvement for Retinex-based methods [7], [17]–[22], [27]. These methods can make the enhancement effect more significant, but the execution time is too long to be conducive to real-time processing.

Fusion-based algorithms have been widely used for image enhancement, which blend several enhanced images by

The associate editor coordinating the review of this manuscript and approving it for publication was Andrea F. Abate.

different methods into a single one. In [23] and [24], two fusion-based methods are developed to improve the quality of low-light images. However, the contrast in bright regions isn't high enough. In [44], a new single-image dehazing solution is proposed based on the adaptive structure decomposition integrated multi-exposure image fusion, which can greatly enhance local details of foggy images. In [45], a novel image fusion framework based on non-subsampled shearlet transform is proposed, which can improve the fusion quality of multi-modal images. In [46], a novel multi-modality medical image fusion method is presented based on phase congruency and local Laplacian energy, which can well preserve structured information and well extract detailed information. The effect of fusion-based method is obvious, and the execution time is not long. However, it is not clear how input images affect the performance during fusion.

Almost these methods still have low contrast within high illuminance regions. In order to enhance the visibility of dark regions and simultaneously achieve high contrast of bright regions for low-light images, this paper proposes a novel enhancement method by fusion. We first define a pair of complementary gamma functions (PCGF). Then, we put forward a new sharpening approach further improve the details and contrast of low-light images. Finally, we design a simple fusion method to merge the value component of the enhanced image in HSV space by PCGF and the value component of the enhanced image in HSV space by sharpening.

The main contributions of this paper can be summarized in following three aspects:

1) We define a pair of complementary gamma functions (PCGF). PCGF can achieve a delicate balance between underexposure and overexposure, so it can greatly improve the contrast of dark regions and bright regions in the image at the same time. Proposed PCGF can hopefully applied in foggy image dehazing, underwater image enhancement and saliency detection and so on.
2) We design a simply and effectively weight summation method based on the average of the value component in HSV space. Either weighting factor is directly proportional to the average value component of the corresponding mapped image derived from PCGF, so the output image can achieve a moderate brightness.
3) We design an image fusion strategy which can achieve excellent enhancement results for low-light images. One input image is derived from PCGF to achieve a satisfactory global contrast and a moderate whole luminance. While the other is derived by combining traditional unsharp masking method and histogram equalization method to further improve local details.

The remainder of this paper is organized as follows. In Section II, we deliver a brief review of traditional gamma correction. In Section III, We then describe the proposed pair of complementary gamma functions (PCGF) and show its outstanding potential by some preliminary experimental results. In Section IV, we detail our low-light image enhancement method based on PCGF by fusion. The experimental results are presented and discussed in Section V. Finally, the conclusion and prospect are given in Section VI.

II. RELATED WORK

The response of cathode ray tubes (CRTs) caused by electrostatic effects in the electron gun or many imaging devices has the following nonlinear output [33]:

$$y = x^{1/\gamma}, \quad 1/\gamma = 2.2 \tag{1}$$

where x and y are the normalized input image and the normalized output image, respectively. Gamma correction (GC) is associated with the above CRT gamma (1) and it is just the inverse of CRT gamma (1) as follows [34]:

$$y = x^{\gamma}, \quad \gamma < 1 \tag{2}$$

where $\gamma < 1$ is a constant, usually taken as $1/2.2$ or 0.4545. For RGB images, the transformation is executed for three channels separately. GC has been frequently used for image enhancement.

Fig. 1 shows two original low-light images and enhanced ones by GC, from which it can be seen that enhanced images have better visual effects on the whole. However, their bright areas are also enlarged which makes them too bright and also reduces the local contrast within high illuminance regions. Obviously, CRT gamma has the opposite effect on low-light images.

FIGURE 1. Low-light image enhancement by GC: (a) original low-light images; (b) enhanced images by GC.

Ju *et al.* propose gamma correction prior (GCP) for dehazing which is described as [31]:

$$y = 1 - (1 - x)^{\gamma}, \quad \gamma < 1 \tag{3}$$

In the process, the input image x is firstly inverted into $1 - x$, then it is processed by GC and finally inverted back to output the processed image y. It is said that the outputs of GC and GCP from haze images are inhomogeneous and homogeneous, respectively. In fact, Dong *et al.* [29] propose the inverse strategy for the first time and then it is used for low-light image enhancement [26], [30].

III. PAIR OF COMPLEMENTARY GAMMA FUNCTIONS

A. PAIR OF COMPLEMENTARY GAMMA FUNCTIONS (PCGF)

From Fig. 1, it is obvious that GC can improve the overall brightness of low-light images, but the bright area is also

increased which makes the enhanced image too bright and perhaps still has poor visibility. Therefore, GC is often used as a preprocessing step. Fig. 2 gives some original low-light images and their two corresponding maps by CRT gamma (1) and GC (2), from which it can be seen that the CRT gamma (1) can make image edge and contour clear while the inverse GC (2) can make low-illumination regions become visible.

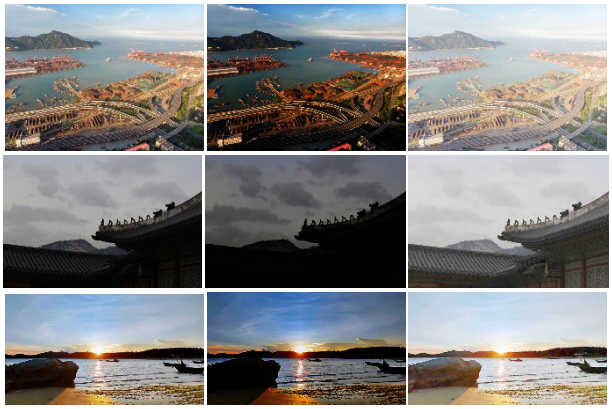

FIGURE 2. Maps of original low-light images by GC and CRT gamma: (a) original low-light images; (b) CRT gamma (1); (c) GC (2).

Inspired by (3), we define a new function as follows:

$$y = 1 - (1 - x)^{1/\gamma}, \quad \gamma < 1 \tag{4}$$

Mapping the right side of (4) by the traditional GC, we can derive the following function:

$$y = \left(1 - (1 - x)^{1/\gamma}\right)^{\gamma}, \quad \gamma < 1 \tag{5}$$

Fig. 3 shows two original low-light images and their corresponding maps by (2)-(5), respectively. From Figs. 3 (a) and (b), it can be seen that the enhanced images by GC still haven't abundant details and satisfactory contrast. From Figs. 3 (a) and (c), it can be found that the output image by (3) is darker than the original low-light images. While from Figs. 3 (a) and (e), it can be found that the output image by (5) is brighter than the original low-light images.

The following is a qualitative analysis from the perspective of function. All the below analysis is based on the premise of $x \in (0, 1)$. First of all, for $\varepsilon < 0$, the power exponent function $y = x^{\varepsilon}$ satisfies that:

$$y = x^{\varepsilon} > 1$$

In other words, for $\kappa_1 < \kappa_2$, the power exponent function $y = x^{\kappa_1}$ satisfies that:

$$x^{\kappa_1} > x^{\kappa_2}$$

Hence, for $\gamma < 1$, we have for GC (2):

$$y = x^{\gamma} > x \tag{6}$$

and

$$(1 - x)^{\gamma} > 1 - x \tag{7}$$

Therefore, we can further obtain:

$$y = 1 - (1 - x)^{\gamma} < 1 - (1 - x) = x \tag{8}$$

As a result, the mapping defined by (3) makes any low-light image much darker than the original low-light image and the output can be seen its underexposed version.

Likewise, for $\gamma < 1$, we have for CRT gamma (1):

$$(1 - x)^{1/\gamma} < 1 - x \tag{9}$$

Therefore, we have

$$y = 1 - (1 - x)^{1/\gamma} > 1 - (1 - x) = x \tag{10}$$

Finally, from (6) and (10), we can get:

$$y = \left(1 - (1 - x)^{1/\gamma}\right)^{\gamma} > x^{\gamma} > x \tag{11}$$

As a result, the mapping defined by (5) makes any low-light image much brighter than GC and the output can be seen its overexposed version.

From the above results and analysis, we can see that there is a complementary relationship between (3) and (5), so in order to better enhance low-light images and achieve a delicate balance, we can integrate them into an intrinsic whole and thus construct the following pair of complementary gamma functions (PCGF):

$$\begin{cases} y_1 = 1 - (1 - x)^{\gamma} \\ y_2 = \left(1 - (1 - x)^{1/\gamma}\right)^{\gamma} \end{cases} \tag{12}$$

We will hopefully obtain moderate exposed images with high quality by the above PCGF (12).

B. IMAGE ENHANCEMENT BY PCGF

By naïve blending strategy, we can derive the final enhanced image:

$$y = c_1 y_1 + c_2 y_2 \tag{13}$$

where y_i is the mapped image from the original low-light image according to (12) and the weighting factor is determined by:

$$c_i = \frac{\overline{V}_i}{\sum_i \overline{V}_i} \tag{14}$$

where $\bar{V}_i$ is the average value of mapped image y_i in HSV space. Since either weighting factor is directly proportional to the average value component of the corresponding mapped image, the output image will have a moderate brightness.

Figs. 4(a) and 4(b) show the corresponding enhanced images of those low-light images shown in Fig. 3(a) by PCGF which is performed on all RGB channels and only on the value component (V) in HSV space, respectively. In Fig. 4(a), all RGB channels of any original low-light image are mapped by PCGF (12). Then the enhanced image is obtained according to (13) and (14). While in Fig. 4(b), any low-light image is firstly transformed from RGB space to HSV space, the value component is mapped by PCGF (12), then two obtained value

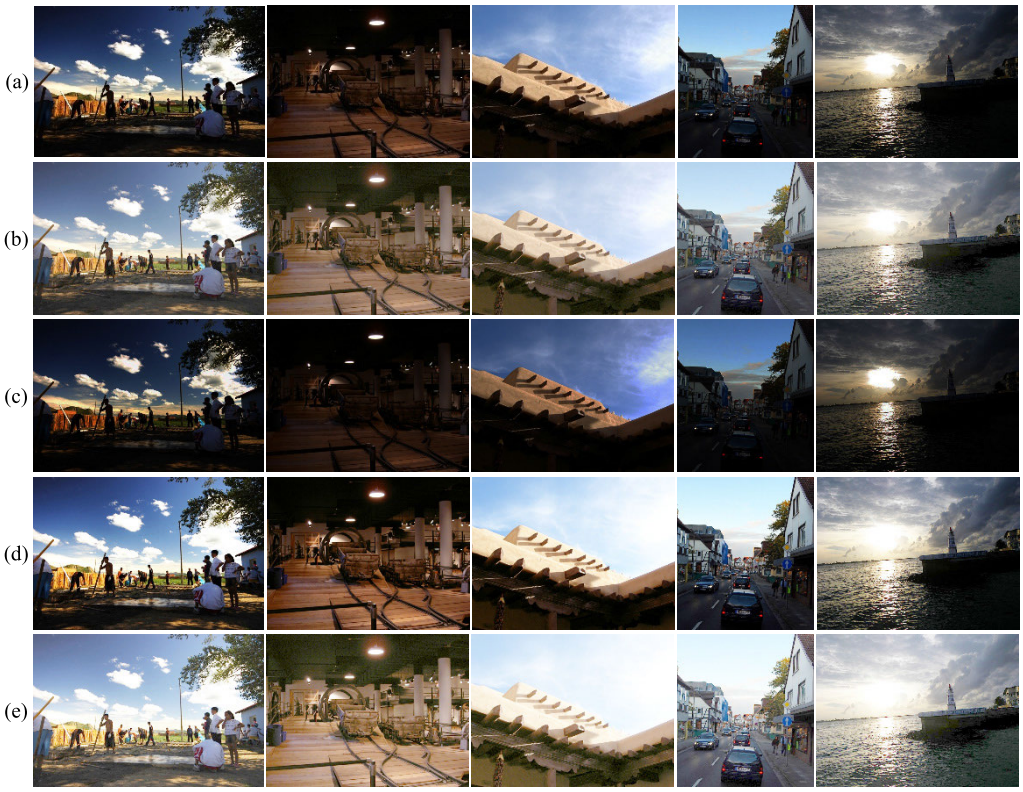

FIGURE 3. Maps of original low-light image by different functions: (a) original low-light images; (b) GC: $y = x^{\gamma}, \gamma < 1$ (2); (c) $y = 1 - (1 - x)^{\gamma}, \gamma < 1$ (3); (d) $y = 1 - (1 - x)^{1/\gamma}, \gamma < 1$ (4); (e) $y = \left(1 - (1 - x)^{1/\gamma}\right)^{\gamma}$, $\gamma < 1$ (5).

components are added according to (13) and (14) to output the value component in HSV space. Finally, the previous obtained value component (V), together with the hue component (H) and the saturation component (S) of the original low-light image, is transformed back to RGB space, and the desired enhanced RGB image is finally output.

It can be seen from Fig. 4 that mapping V in HSV space achieves better visual results than independently mapping all RGB channels. In fact, HSV color space provides a good color representation for human perception and can completely separate color information from brightness information, as means that the original color of any pixel will not be influenced by any processing of the value component [43]. Thus we will only treat the value component in HSV space during the fusion process in the next section.

IV. LOW-LIGHT IMGAE ENHANCEMENT BASED ON PCGF BY FUSION

From Fig. 4, it can be seen that PCGF can effectively enhance low-light images. It not only significantly improves the overall brightness of low-light images, but also enhances the details by stretching the dark regions and compressing the bright regions to a certain extent. However, the details and local contrast are still not prominent enough. To further improve the quality, we build on a simple fusion strategy. Image fusion is widely used for low-light image enhancement [23], [24], underwater image enhancement [32], image dehazing [44], multi-focus image processing [45], [46] and so on. Similar to [23] and [24], our approach is to blend a set of inputs and weight maps derived from a single original low-light image, which contains three main steps: deriving input images for fusion, defining weight maps, and fusing of the input images incorporating the defined weight maps.

The whole flow chart of proposed low-light image enhancement method based on PCGF by fusion is illustrated by Fig. 5. The value component (V) of an original low-light image is firstly processed by gamma enhancement according to (13) and by detail enhancement according to (19) which will be presented below, then two obtained value components are fused by the Laplace pyramids method shown as in (22) below. The value component (V) resulting from the fusion process and the hue component (H) and the saturation component (S) of the original low-light image are together transformed back to RGB space to output the desired enhanced RGB image.

In the following, we will show how to obtain input images for fusion and the corresponding weight maps and will also illustrate the fusion process in detail.

A. INPUT IMAGES FOR FUSION

The first input (I_1) for fusion is directly derived from the enhanced value component of the original low-light image in HSV space by PCGF according to (13) and (14).

The second input (I_2) for fusion is derived from the enhanced version of the original low-light image through combining sharpening and histogram equalization (HE).

FIGURE 4. Enhanced images of low-light images shown in Fig. 3 (a) by (7): (a) mapping RGB channels; (b) mapping the value component in HSV space.

Image sharpening such as unsharp masking (UM) and classical HE are commonly used to improve details and contrast of low-light images, respectively. The typical formula for UM is as follows [39]–[41]:

$$S = I + \alpha \cdot (I - G * I) \tag{15}$$

where I and S are the input image and sharpened image, respectively; G is a Gaussian kernel function; α is a preset constant to control the level of contrast enhancement which is selected between 0.5 and 1.5; $*$ denotes the convolution operation. Some improved UM methods have been proposed in [40] and [41]. In [40], an adaptive sharpening strength selection method is given. While in [41] a pixel-wise method for enhancement strength is determined according to local blurriness measure of the original input image. However, if we only perform the sharpening procedure, image details will not be significantly enhanced due to the overall darkness of low-light images.

In the following we will design a strategy to obtain the second input image for fusion by combining traditional UM method and HE method. Setting $\alpha = 1$ in traditional UM (15), we can get:

$$S_1 = V + (V - G * V) \tag{16}$$

where V represents the value component of the original low-light image in HSV space. However, UM itself isn't inadequate and doesn't work fine for low-light images, so we can improve the contrast by executing HE on V in (16) and hence we have:

$$S_2 = 2H(V) - G * H(V) \tag{17}$$

where $H(\cdot)$ denotes the HE operation. In order to further reduce artifacts, we can average the value component V and the above obtained S_2 and hence derive the second input image for fusion:

$$I_2 = \frac{V + S_2}{2} \tag{18}$$

Finally, we have the second input image for fusion:

$$I_2 = (V + 2H(V) - G * H(V))/2 \tag{19}$$

B. WEIGHT MAPS FOR FUSION

Light exposure has great impact on images' quality. Therefore, we select exposedness weight map to obtain regions with good exposure from input images for fusion. Exposedness weight map is utilized in [23], [24] and [32] to evaluate the degree of exposure, which is expressed as a Gaussian-modeled distance to the average normalized range value 0.5 as follows:

$$w_i(x, y) = \exp\left\{-\frac{(I_i(x, y) - 0.5)^2}{2 \times 0.25^2}\right\} \tag{20}$$

where $I_i(x, y)$ represents the ith input image with the pixel location (x, y). Fu *et al.* [23] conducted many experiments on 2000 images and found that the average of the mean values approximately equals 0.5 and the average of the standard deviations approximately equals 0.25. So the above exposedness weight map is reasonable. Higher values will be assigned to those pixels which are close to 0.5. This kind of weight map assigns small values to pixels with under-exposed and over-exposed regions while normal-exposed pixels obtain high values. Hence, it achieves an unbiased assignment.

Finally, the normalized weight maps for fusion are given by:

$$\overline{w}_i(x, y) = \frac{w_i(x, y)}{\sum_i w_i(x, y)} \tag{21}$$

C. IMGAE FUSION PROCESS

In order to overcome undesirable halos and artifacts resulting from naive blending for fusion, we employ the pyramid fusion proposed by Burt and Adelson [35]. Both input images are decomposed into Laplace pyramids, while both corresponding weight maps are decomposed into Gaussian pyramids. Then blend Laplacian inputs and Gaussian weight maps of each level. Finally, the enhanced image is given by:

$$I_{output}(x, y) = \sum_l U_d\left(\sum_{i=1}^{2} G^l(\overline{w}_i(x, y)) L^l(I_i(x, y))\right) \tag{22}$$

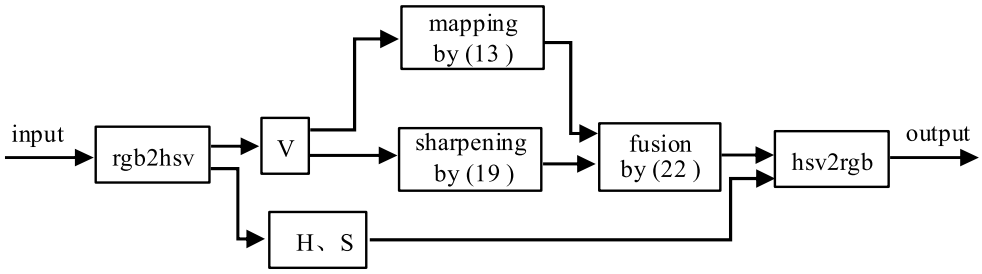

FIGURE 5. Flow chart of proposed low-light image enhancement method based on pair of complementary gamma-correction functions by fusion.

where l represents the number of layers of the pyramids, U_d is the up-sampling operator with $d = 2^l - 1$, $G(\cdot)$ and $L(\cdot)$ represent Gaussian operator and Laplace operator, respectively. By a large number of experiments, we find that decomposition into four layers can achieve excellent performance with low calculation load.

V. EXPERIMENTS AND DISCUSSION

In this section, we evaluate the performance of the proposed method. First, we present our experiment settings. Then, we evaluate the proposed method by comparing it with other state-of-the-art methods in both subjective and objective aspects.

A. EXPERIMENTS PREPARATIONS

To fully evaluate the proposed method, one hundred images with low illumination from various scenes have been tested. Test images come from Lee and Kim [6], Fu *et al.* [23], Wang *et al.* [24], Guo *et al.* [26], and our team. All images are processed in MATLAB R2017b on a PC running Windows 10 OS with 32G RAM and 2.1GHz CPU.

The methods for comparison include global contrast enhancement method based on the layered difference representation (CE) [6], efficient contrast enhancement using adaptive gamma correction with weighting distribution (AGCWB) [7], fusion-based enhancement method (FE) [23], bio-inspired multi-exposure fusion framework (BIMEF) [25], low-light image enhancement via illumination map estimation (LIME) [26], structure-revealing low-light image enhancement via robust Retinex model (SRM) [27], low-light image enhancement using the camera response model (LECARM) [28] and the proposed PCGF method.

B. SUBJECTIVE EVALUATION

Three low-light images, which are named *Street*, *Sea* and *Church* are shown in Fig. 6(a) from left to right. Figs. 6(b) to 6(h) successively illustrate the enhanced results from CE [6], AGCWB [7], FE [23], BIMEF [25], LIME [26], SRM [27], LECARM [28] and the proposed PCGF method. Some zoom-in detailed patches are also shown on the right of each enhanced image. From Fig. 6, we can find that LIME causes color distortion; output images by FE are somewhat over-enhancement; the whole brightness by both CE and AGCWB is still insufficient; the enhanced *Sea* image by BIMEF has a faint halo round the sun and the enhanced *Church* image by BIMEF has a faint halo near upper right of the roof; the enhanced *Sea* image by SRM has low local details outside of the ship; the light in all three enhanced images by LECARM is not well focused. Meanwhile, it can be seen that for the *Street* image, our enhanced image has sharp focus of the light beam on the left of the woman and clear leaves. For the *Sea* image, our enhanced image has clear outline around the sun and moderate texture outside of the ship. For the *Church* image, our enhanced image has clear contour for the cloud behind the cross on the roof and it has clear edge on the roof. By and large, our method can preserve image details and naturalness effectively.

The enhancement results of other five low-light images by the above different methods are shown in Fig. 7. We can find that enhanced images by CE are still a little dark and have poor visual quality. Enhanced images by AGCWD don't preserve details in bright regions, for example the crane's feather in the *Crane* image. BIMEF is effective in preserving the naturalness, but enhanced images are also a little dark. LIME can effectively improve the overall brightness. However, some regions such as the trees in the *Walkway* image and the *Crane* image suffer from over-enhancement. The details of enhanced image by SRM are not prominent enough. Our method achieves excellent visibility, contrast and details and the whole images have moderate brightness. While enhanced images by FE are a bit unnatural; and the enhanced images by LECARM are more or less over-exposed, whose details are slightly inferior to our method.

C. OBJECTIVE EVALUATION

Besides the subjective visual appearance and to further explain the effectiveness of our method, we employ NIQE [36], ILNIQE [37], SSEQ [38], and BRISQUE [42] to objectively evaluate the results of our method. These no-reference metrics are widely used for performance evaluation in the field of low-light image enhancement. A brief introduction is made for them in the following.

NIQE (Natural Image Quality Evaluator) assesses image quality without any knowledge of distortions or human opinions of them through constructing several quality-aware

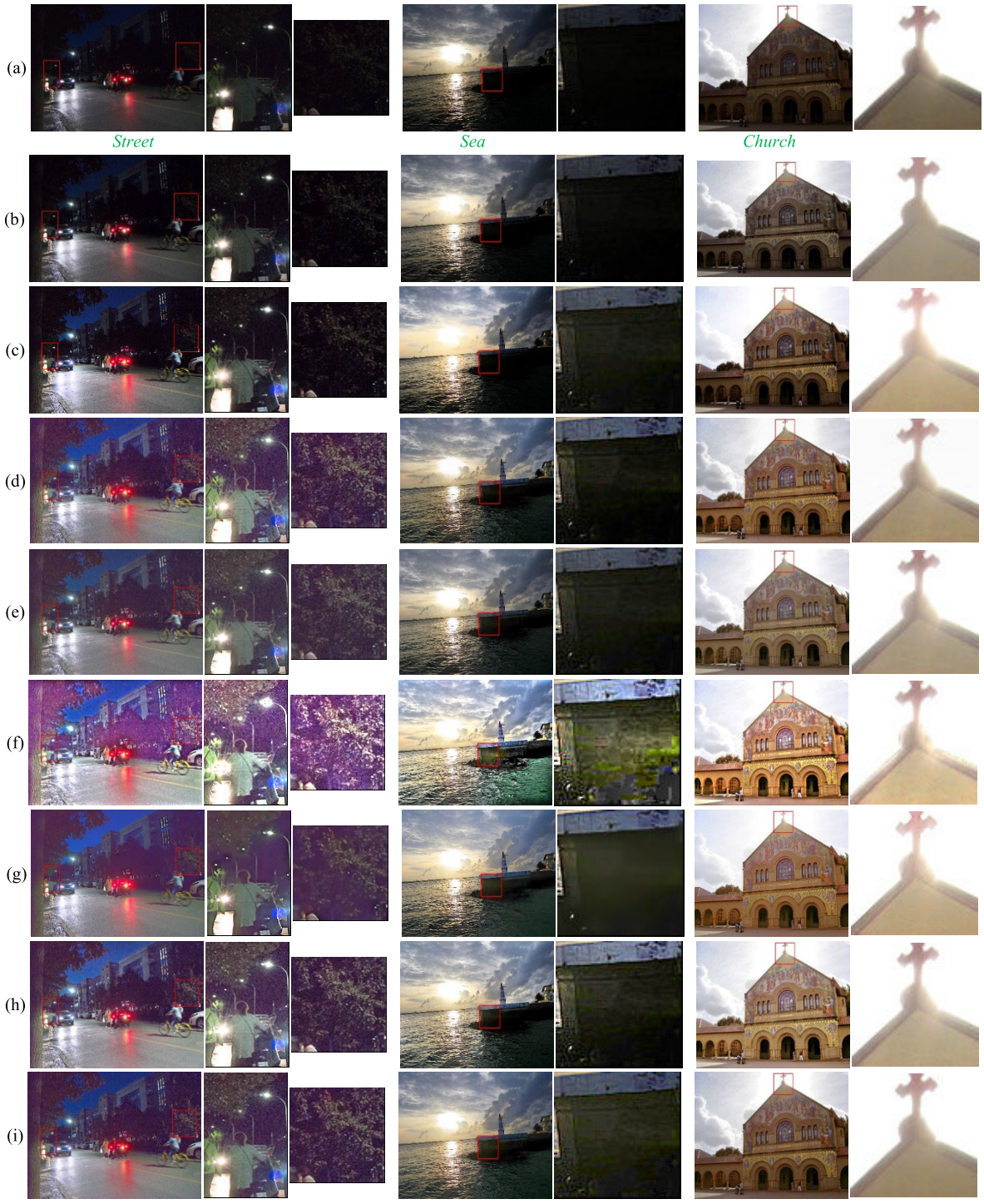

FIGURE 6. Low-light image enhancement results by different methods: (a) original images: ***Street, Sea*** and ***Church*** from left to right; (b) CE [6]; (c) AGCWB [7]; (d) FE [23]; (e) BIMEF. [25]; (f) LIME [26]; (g) SRM [27]; (h) LECARM [28]; (i) proposed PCGF.

statistical features based on the natural scene statistic model. ILNIQE (Integrated Local NIQE) can comprehensively capture local distortion artifacts through integrating quality-aware features by a local multivariate Gaussian model. SSEQ, which is a Spatial-Spectral Entropy-based Quality index, can assess distorted image's quality and achieve very good predictive performance. BRISQUE (Blind/Referenceless Image Spatial Quality Evaluator) quantifies naturalness losses resulting from distortions by using scene statistics of locally normalized luminance coefficients in the image. The smaller all these indexes, the better the performance. Besides, values for PSNR (Peak Signal-to-Noise Ratio) are also given.

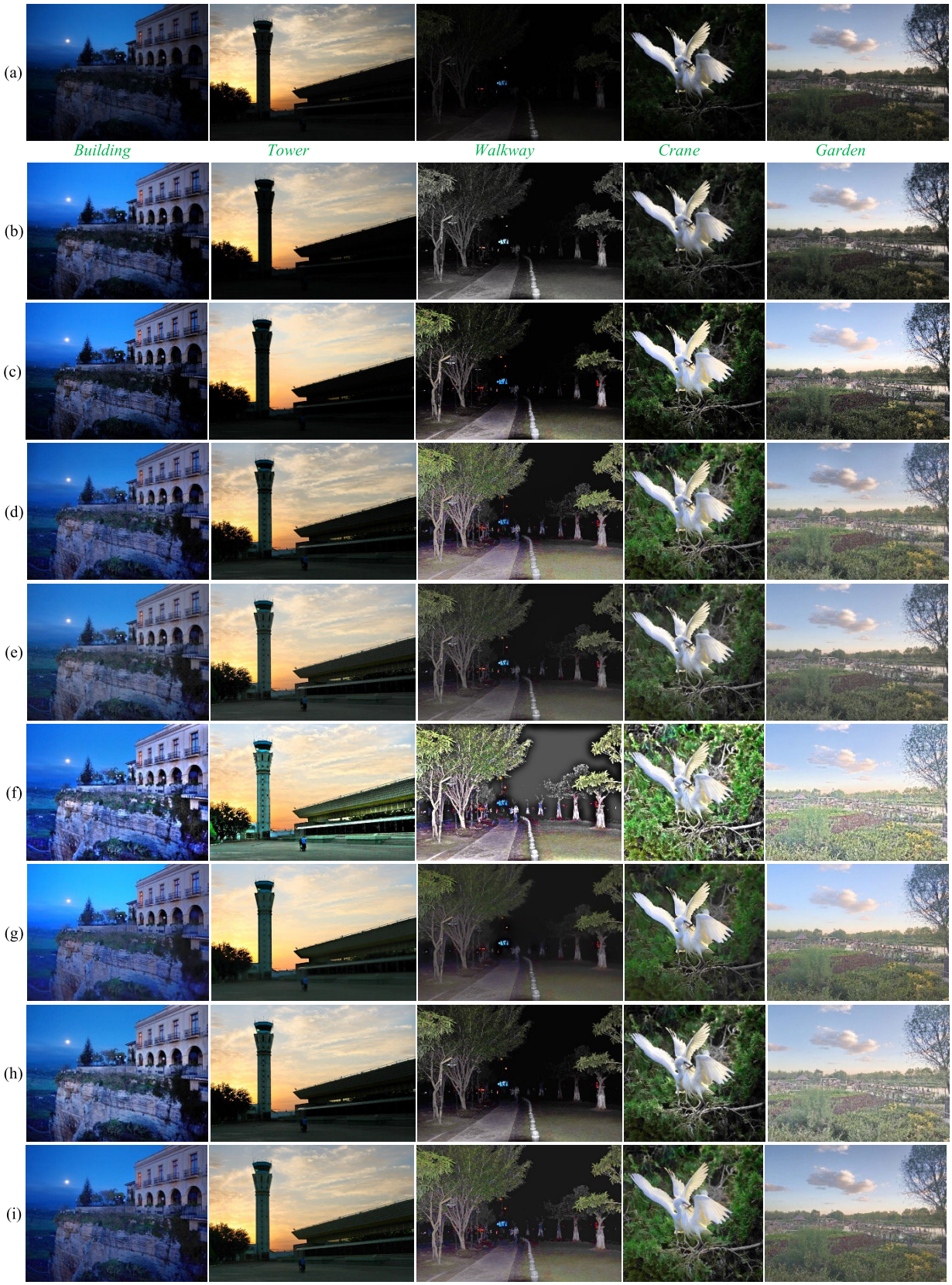

FIGURE 7. Low-light image enhancement results by different methods: (a) original images: *Building, Tower, Walkway, Crane and Garden* from left to right; (b) CE [6]; (c) AGCWB [7];(d) FE [23]; (e) BIMEF [25]; (f) LIME [26]; (g) SRM [27]; (h) LECARM [28]; (i) proposed PCGF.

TABLE 1. Average quantitative comparison of 100 enhanced images.

Metric	CE [6]	AGCWD [7]	FE [24]	BIMEF [26]	LIME [27]	SRM [28]	LECARM [29]	Ours
NIQE (↓)	3.89	3.85	3.84	3.79	3.72	3.82	3.76	**3.71**
ILNIQE (↓)	26.47	26.97	26.40	26.32	28.76	25.86	26.71	**25.49**
SSEQ (↓)	24.64	23.94	24.27	24.22	24.06	23.35	24.33	**22.86**
BRISQUE (↓)	25.87	25.77	25.91	26.06	25.96	26.12	**25.37**	25.83
PSNR (↑)	**69.47**	65.52	63.79	64.11	57.52	63.82	61.14	64.20

It is obvious that larger value for PSNR means better quality of an enhanced image.

Quantitative results for total 100 images which consist of the same 92 random selected images from and 8 images shown in Figs. 6 and 7 are given in Table 1. It can be seen that our method has the best scores for NIQE, ILNIQE and SSEQ, which means our algorithm has absolute priority in low-light image enhancement to preserve the details, naturalness and reduce artifacts and distortions. Both scores for BRISQUE and PSNR by our method rank third out of eight. LECARM and CE have the best scores for BRISQUE and PSNR, respectively. Objectively speaking, our method can achieve satisfying scores. Overall, our method outperforms almost all other methods and hence is effective for low-light image enhancement.

VI. CONCLUSION

In this paper, we define a pair of complementary gamma functions (PCGF) by which we can obtain an underexposed version and an overexposed version of the original low-light image so that we can combine them to achieve a moderate brightness. We show the outstanding potential of PCGF for low-light image enhancement by some preliminary experimental results. We also design a fusion strategy to release its performance for low-light images based on PCGF. Two input images used for fusion are derived from the enhanced image by PCGF and the enhanced image by proposed sharpening method, respectively. Experiments show that proposed method can significantly enhance the detail and improve the contrast of low-light image. Objective and subjective assessment between different methods show its outperformance. As future work, we plan to develop better fusion methods to achieve its full potential. Besides, we will try to apply the proposed PCGF for foggy image dehazing, underwater image enhancement and saliency detection and so on.

ACKNOWLEDGMENT

The authors would like to thank the anonymous reviewers for their valuable suggestions and helpful comments which have greatly improved the manuscript.

REFERENCES

[1] J. Redmon, S. Divvala, R. Girshick, and A. Farhadi, "You only look once: Unified, real-time object detection," in *Proc. IEEE Conf. Comput. Vis. Pattern Recognit. (CVPR)*, Jun. 2016, pp. 779–788.

[2] J. Wang, W. Wang, R. Wang, and W. Gao, "CSPS: An adaptive pooling method for image classification," *IEEE Trans. Multimedia*, vol. 18, no. 6, pp. 1000–1010, Jun. 2016.

[3] R. Achanta, S. Hemami, F. Estrada, and S. Susstrunk, "Frequency-tuned salient region detection," in *Proc. IEEE Conf. Comput. Vis. Pattern Recognit.*, Jun. 2009, pp. 1597–1604.

[4] P. M. Narendra and R. C. Fitch, "Real-time adaptive contrast enhancement," *IEEE Trans. Pattern Anal. Mach. Intell.*, vol. PAMI-3, no. 6, pp. 656–661, Nov. 1981.

[5] S. M. Pizer, E. P. Amburn, J. D. Austin, R. Cromartie, A. Geselowitz, T. Greer, B. ter Haar Romeny, J. B. Zimmerman, and K. Zuiderveld, "Adaptive histogram equalization and its variations," *Comput. Vis., Graph., Image Process.*, vol. 39, no. 3, pp. 355–368, 1987.

[6] C. Lee, C. Lee, and C.-S. Kim, "Contrast enhancement based on layered difference representation of 2D histograms," *IEEE Trans. Image Process.*, vol. 22, no. 12, pp. 5372–5384, Dec. 2013.

[7] S.-C. Huang, F.-C. Cheng, and Y.-S. Chiu, "Efficient contrast enhancement using adaptive gamma correction with weighting distribution," *IEEE Trans. Image Process.*, vol. 22, no. 3, pp. 1032–1041, Mar. 2013.

[8] T. Celik and T. Tjahjadi, "Contextual and variational contrast enhancement," *IEEE Trans. Image Process.*, vol. 20, no. 12, pp. 3431–3441, Dec. 2011.

[9] H. Xu, G. Zhai, X. Wu, and X. Yang, "Generalized equalization model for image enhancement," *IEEE Trans. Multimedia*, vol. 16, no. 1, pp. 68–82, Jan. 2014.

[10] C. Lee, C. Lee, Y.-Y. Lee, and C.-S. Kim, "Power-constrained contrast enhancement for emissive displays based on histogram equalization," *IEEE Trans. Image Process.*, vol. 21, no. 1, pp. 80–93, Jan. 2012.

[11] T. Celik, "Spatial entropy-based global and local image contrast enhancement," *IEEE Trans. Image Process.*, vol. 23, no. 12, pp. 5298–5308, Dec. 2014.

[12] U. K. Nafis, K. V. Arya, and M. Pattanaik, "Histogram statistics based variance controlled adaptive threshold in anisotropic diffusion for low contrast image enhancement," *Signal Process.*, vol. 93, no. 6, pp. 1684–1693, Jun. 2013.

[13] E. H. Land, "The retinex theory of color vision," *Sci. Amer.*, vol. 237, no. 6, pp. 108–128, Dec. 1977.

[14] D. J. Jobson, Z. Rahman, and G. A. Woodell, "Properties and performance of a center/surround retinex," *IEEE Trans. Image Process.*, vol. 6, no. 3, pp. 451–462, Mar. 1997.

[15] D. J. Jobson, Z. Rahman, and G. A. Woodell, "A multiscale retinex for bridging the gap between color images and the human observation of scenes," *IEEE Trans. Image Process.*, vol. 6, no. 7, pp. 965–976, Jul. 1997.

[16] M. Elad, R. Kimmel, D. Shaked, and R. Keshet, "Reduced complexity retinex algorithm via the variational approach," *J. Vis. Commun. Image Represent.*, vol. 14, no. 4, pp. 369–388, Dec. 2003.

[17] Q. Zhao, P. Tan, Q. Dai, L. Shen, E. Wu, and S. Lin, "A closed-form solution to retinex with nonlocal texture constraints," *IEEE Trans. Pattern Anal. Mach. Intell.*, vol. 34, no. 7, pp. 1437–1444, Jul. 2012.

[18] X. Fu, Y. Liao, D. Zeng, Y. Huang, X.-P. Zhang, and X. Ding, "A probabilistic method for image enhancement with simultaneous illumination and reflectance estimation," *IEEE Trans. Image Process.*, vol. 24, no. 12, pp. 4965–4977, Dec. 2015.

[19] B. Cai, X. Xu, K. Guo, K. Jia, B. Hu, and D. Tao, "A joint intrinsic-extrinsic prior model for retinex," in *Proc. IEEE Int. Conf. Comput. Vis. (ICCV)*, Oct. 2017, pp. 4000–4009.

[20] Z. Liang, J. Xu, D. Zhang, Z. Cao, and L. Zhang, "A hybrid l1-l0 layer decomposition model for tone mapping," in *Proc. IEEE/CVF Conf. Comput. Vis. Pattern Recognit.*, Jun. 2018, pp. 4758–4766.
[21] J. Wang, W. Tan, X. Niu, and B. Yan, "RDGAN: Retinex decomposition based adversarial learning for low-light enhancement," in *Proc. IEEE Int. Conf. Multimedia Expo (ICME)*, Jul. 2019, pp. 1186–1191.
[22] J. Xu, Y. Hou, D. Ren, L. Liu, F. Zhu, M. Yu, H. Wang, and L. Shao, "STAR: A structure and texture aware retinex model," *IEEE Trans. Image Process.*, vol. 29, pp. 5022–5037, Mar. 2020.
[23] X. Fu, D. Zeng, Y. Huang, Y. Liao, X. Ding, and J. Paisley, "A fusion-based enhancing method for weakly illuminated images," *Signal Process.*, vol. 129, pp. 82–96, Dec. 2016.
[24] Q. Wang, X. Fu, X.-P. Zhang, and X. Ding, "A fusion-based method for single backlit image enhancement," in *Proc. IEEE Int. Conf. Image Process. (ICIP)*, Sep. 2016, pp. 4077–4081.
[25] Z. Ying, G. Li, and W. Gao, "A bio-inspired multi-exposure fusion framework for low-light image enhancement," 2017, *arXiv:1711.00591*. [Online]. Available: http://arxiv.org/abs/1711.00591
[26] X. Guo, Y. Li, and H. Ling, "LIME: Low-light image enhancement via illumination map estimation," *IEEE Trans. Image Process.*, vol. 26, no. 2, pp. 982–993, Feb. 2017.
[27] M. Li, J. Liu, W. Yang, X. Sun, and Z. Guo, "Structure-revealing low-light image enhancement via robust retinex model," *IEEE Trans. Image Process.*, vol. 27, no. 6, pp. 2828–2841, Jun. 2018.
[28] Y. Ren, Z. Ying, T. H. Li, and G. Li, "LECARM: Low-light image enhancement using the camera response model," *IEEE Trans. Circuits Syst. Video Technol.*, vol. 29, no. 4, pp. 968–981, Apr. 2019.
[29] X. Dong, Y. Pang, and J. Wen, "Fast efficient algorithm for enhancement of low lighting video," in *Proc. ACM SIGGRAPH Posters (SIGGRAPH)*, 2010, pp. 1–6.
[30] L. Li, R. Wang, W. Wang, and W. Gao, "A low-light image enhancement method for both denoising and contrast enlarging," in *Proc. IEEE Int. Conf. Image Process. (ICIP)*, Sep. 2015, pp. 3730–3734.
[31] M. Ju, C. Ding, Y. J. Guo, and D. Zhang, "IDGCP: Image dehazing based on gamma correction prior," *IEEE Trans. Image Process.*, vol. 29, pp. 3104–3118, Dec. 2020.
[32] C. O. Ancuti and C. Ancuti, "Single image dehazing by multi-scale fusion," *IEEE Trans. Image Process.*, vol. 22, no. 8, pp. 3271–3282, Aug. 2013.
[33] C. A. Poynton, "SMPTE tutorial: 'Gamma' and its disguises: The nonlinear mappings of intensity in perception, CRTs, film, and video," *SMPTE J.*, vol. 102, no. 12, pp. 1099–1108, Dec. 1993.
[34] S. Mann, "Comparametric equations with practical applications in quantigraphic image processing," *IEEE Trans. Image Process.*, vol. 9, no. 8, pp. 1389–1406, Aug. 2000.
[35] P. Burt and E. Adelson, "The Laplacian pyramid as a compact image code," *IEEE Trans. Commun.*, vol. 31, no. 4, pp. 532–540, Apr. 1983.
[36] A. Mittal, R. Soundararajan, and A. C. Bovik, "Making a 'Completely Blind' image quality analyzer," *IEEE Signal Process. Lett.*, vol. 20, no. 3, pp. 209–212, Mar. 2013.
[37] L. Zhang, L. Zhang, and A. C. Bovik, "A feature-enriched completely blind image quality evaluator," *IEEE Trans. Image Process.*, vol. 24, no. 8, pp. 2579–2591, Aug. 2015.
[38] L. Liu, B. Liu, H. Huang, and A. C. Bovik, "No-reference image quality assessment based on spatial and spectral entropies," *Signal Process., Image Commun.*, vol. 29, no. 8, pp. 856–863, Sep. 2014.
[39] F. Ding, G. Zhu, J. Yang, J. Xie, and Y.-Q. Shi, "Edge perpendicular binary coding for USM sharpening detection," *IEEE Signal Process. Lett.*, vol. 22, no. 3, pp. 327–331, Mar. 2015.
[40] W. Ye and K.-K. Ma, "Blurriness-guided unsharp masking," *IEEE Trans. Image Process.*, vol. 27, no. 9, pp. 4465–4477, Sep. 2018.
[41] A. Polesel, G. Ramponi, and V. J. Mathews, "Image enhancement via adaptive unsharp masking," *IEEE Trans. Image Process.*, vol. 9, no. 3, pp. 505–510, Mar. 2000.
[42] A. Mittal, A. K. Moorthy, and A. C. Bovik, "No-reference image quality assessment in the spatial domain," *IEEE Trans. Image Process.*, vol. 21, no. 12, pp. 4695–4708, Dec. 2012.
[43] N. A. Ibraheem, M. Hasan, R. Z. Khan, and P. K. Mishra, "Understanding color models: A review," *ARPN J. Sci. Technol.*, vol. 2, no. 3, pp. 265–275, Apr. 2012.
[44] M. Zheng, G. Qi, Z. Zhu, Y. Li, H. Wei, and Y. Liu, "Image dehazing by an artificial image fusion method based on adaptive structure decomposition," *IEEE Sensors J.*, vol. 20, no. 14, pp. 8062–8072, Jul. 2020.
[45] S. Liu, J. Wang, Y. Lu, H. Li, J. Zhao, and Z. Zhu, "Multi-focus image fusion based on adaptive dual-channel spiking cortical model in non-subsampled shearlet domain," *IEEE Access*, vol. 7, pp. 56367–56388, 2019.
[46] S. Liu, Y. Lu, J. Wang, S. Hu, J. Zhao, and Z. Zhu, "A new focus evaluation operator based on max–min filter and its application in high quality multi-focus image fusion," *Multidimensional Syst. Signal Process.*, vol. 31, no. 2, pp. 569–590, Apr. 2020.

CHANGLI LI received the B.S. degree in physics from Fudan University, Shanghai, China, in 1999, and the M.S. degree in communication and information systems and the Ph.D. degree in signal and information processing from Xidian University, Xi'an, China, in 2004 and 2010, respectively. Since 2012, he has been an Associate Professor with Hohai University, Nanjing, China. His research interests include image enhancement, blind source separation, and frequency diverse arrays.

SHIQIANG TANG received the B.S. degree in communication engineering from Hohai University, Nanjing, China, in 2019, where he is currently pursuing the M.S. degree in signal and information processing engineering. His research interest includes image enhancement.

JINGWEN YAN received the B.S. degree in electronics engineering from the Jilin University of Technology, Jilin, China, in 1987, the M.Sc. degree in cartography and remote sensing from the Changchun Institute of Geography, Chinese Academy of Sciences, Changchun, China, in 1992, and the Ph.D. degree in optics from the Changchun Institute of Optics, Chinese Academy of Sciences, in 1997. Since 2006, he has been a Professor with the School of Engineering, Shantou University, Shantou, China. His current research interests include digital image processing and compressed sensing.

TENG ZHOU received the B.E. degree in information and computing science from South China Normal University, Guangzhou, China, in 2010, the M.E. degree in computer technology from Sun Yat-sen University, Guangzhou, in 2012, and the Ph.D. degree in computer application technology from the South China University of Technology, Guangzhou, in 2017. He is currently an Associate Professor with the Department of Computer Science, Shantou University, and is also a Research Associate with the Center of Smart Health, The Hong Kong Polytechnic University. His research interests include intelligent transportation systems, image processing, and machine learning and its applications.